Modulation of Intense Relativistic Electron Beams by an External Microwave Source

M. Friedman and V. Serlin
Plasma Physics Division, Naval Research Laboratory, Washington, D.C., 20375
(Received 10 June 1985)

A novel mechanism capable of efficiently modulating intense relativistic electron beams is reported. This mechanism uses unique properties of slow and fast charge-density waves on an intense beam of a finite transverse dimension. The mechanism was investigated with use of an external microwave energy to excite these waves on a beam. Large-amplitude coherent and monochromatic current oscillations were detected on the electron beam at the same frequency as the external source. With use of this mechanism it becomes possible to construct efficient microwave amplifiers suitable for large rf accelerators.

PACS numbers: 41.80.−y, 52.75.−d

The accelerator community is in search of an rf amplifier[1] capable of delivering $\gtrsim 10^9$ W of power at pulse lengths of 100 nsec to 1 μsec for the purpose of driving large rf accelerators. At present, rf accelerators are being powered by klystron amplifiers[2] which modulate a low-voltage–low-current electron beam and extract rf energy from the electron bunches.

A new mechanism capable of completely modulating an intense relativistic electron beam (IREB) of power $\gtrsim 10^9$–10^{10} W was recently discussed.[3] Monochromatic rf energy at a power level of ~ 1 GW was extracted from a bunched electron beam.[4,5]

Using particle simulation techniques we showed[6] that this mechanism can be used to construct an rf amplifier or a phase-locked oscillator. This prediction has been verified experimentally and is reported in this Letter. We found that the interaction between an IREB and an externally generated rf energy led to a large-amplitude monochromatic and coherent oscillation on the IREB current. This beam modulation can be used to generate high-power microwave pulses suitable for accelerator research.

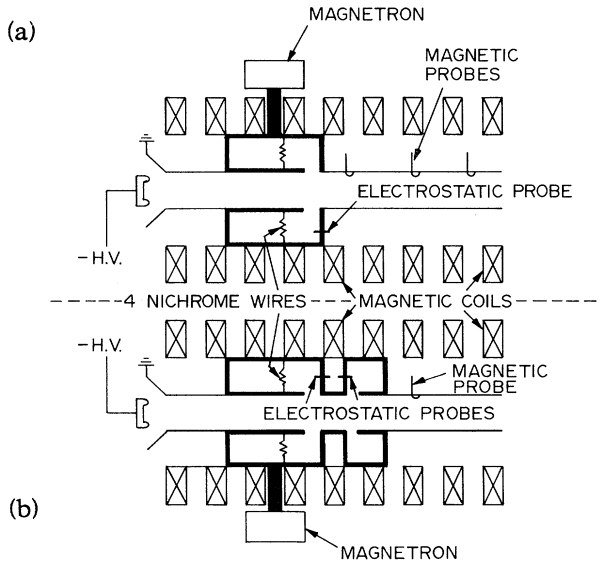

FIG. 1. (a) Experimental arrangement with one cavity. (b) Experimental arrangement with two cavities.

The experimental arrangement shown in Fig. 1(a) consisted of a foilless diode emitting an annular IREB of radius $r_b \simeq 1.9$ cm and thickness $\simeq 0.3$ cm. A 10-kG quasi-dc magnetic field confined the IREB inside a metal tube of radius $r_w \simeq 2.35$ cm. A gap feeding a coaxial cavity was inserted in the drift tube. The characteristic impedance of the cavity was $Z = 45\ \Omega$ and its length was $L = 17$ cm corresponding to a resonance frequency of 410 MHz. Four thin Nichrome wires connected the inner wall of the coaxial cavity to its outer wall so as to reduce the Q of the cavity at 410 MHz. The wires did not influence the Q of the cavity at the 1328-MHz resonance ($Q > 1000$). The presence of the wires shifted the first resonance from 410 to 610 MHz and reduced the Q to below 30. An external rf source (a magnetron) "pumped" microwave energy into the cavity for a duration of 3 μsec at a frequency $f = 1328$ MHz. Sometime during the 3-μsec period a Blumlein transmission line with an output of 500 kV energized the foilless diode for 120 nsec, and an ~ 5-kA electron beam was launched through the drift region. The base pressure in the drift region was $\lesssim 10^{-5}$ Torr. The electron beam was diagnosed by magnetic probes. The voltage at the gap of the cavity was measured by an electrostatic probe. All the probes were calibrated at different frequencies (up to 1.3 GHz). A Tektronix digitizer system analyzed the signal taking into account the attenuations and sensitivities of the probes, cables, attenuators, amplifiers, etc.

The dI/dt signal was Fourier analyzed and integrated to obtain the ac oscillation and current profile. Figure 2 shows examples of the spectra and current profiles. (Note that as a result of the discrete nature of the signal acquisition the fast-Fourier-transform spectrum has an error of ± 50 MHz.)

A summary of the experimental results is given below:

(1) The input power injected into the cavity was 50–100 kW at 1.328 GHz.

(2) Modulation of the current of the IREB was observed at a distance of 5 cm from the gap of the cavity (which was the closest location allowed by the geometry) and remained constant during the 120 nsec of the IREB propagation (Fig. 2).

(3) The depth of current modulation was $\sim 5\%$ at 5 cm downstream, increased to a maximum of 10% at 30 cm, and dropped back to 5% at a distance of 55 cm downstream of the gap.

(4) The phase variation and the frequency of the modulation was measured by mixing the magnetic probe signal with the driving rf signal. The phase varied less than 4° during the pulse duration and the frequency was equal to the driver frequency. These results were the limits of our measuring techniques. The phase difference between the signals of the input and the first magnetic loop did not change on successive pulses.

The results can be explained using linear arguments. A small-signal analysis[3,6] showed that when a voltage $V_1 = V_{10}\exp(j\omega t)$ is applied on an IREB of current I_0 and voltage V_0 at a point $z=0$, slow and fast charge-density waves will be generated. The slow and fast waves combine to generate an ac voltage V_2 and an ac current I_2 at a point z:

$$I_2(z,t) = j[V_{10}/Z(1-\zeta^2)]\{(1+\Psi\zeta)\sin(\alpha\mu\theta) - j(\zeta+\Psi)\cos(\alpha\mu\theta)\}\exp[j(\omega t-\theta)], \tag{1}$$

$$V_2(z,t) = V_{10}[\cos(\alpha\mu\theta) - j\Psi\sin(\alpha\mu\theta)]\exp[j(\omega t-\theta)], \tag{2}$$

where

$$\alpha = [I_0(\mathrm{kA})]\ln(r_w/r_b)/8.5\beta_0\gamma_0^3, \quad \delta = \beta_0^2/(\beta_0^2-\alpha), \quad \alpha\mu = [\alpha^2+\alpha(1-\beta_0^2)]^{1/2}/\beta_0,$$
$$\zeta = (1-\delta)/\alpha\mu\delta, \quad \theta = \omega\delta z/c\beta_0, \quad Z = (V_0/I_0)(mc^2\beta_0^2\gamma_0^3/eV_0)(\alpha\mu), \tag{3}$$

and where Ψ is the relative difference in amplitude of fast and slow waves (e.g., $\Psi=0$ means that the amplitudes of the slow and fast waves are the same), $\beta_0 = u_0/c$, $\gamma_0 = (1-\beta_0^2)^{-1/2}$, and u_0 is the propagating velocity of the electrons, which can be derived from

$$\gamma = \gamma_0 + \alpha\gamma_0^3, \quad \gamma = (eV_0/m_0c^2+1).$$

The kinetic power P_{ak} is

$$P_{ak} = \langle I_1(z,t)V_2^*(z,t)\rangle = [V_{10}^2/Z(1-\zeta^2)][\zeta+\Psi)\cos^2\alpha\mu\theta - (1+\zeta\Psi)\Psi\sin^2\alpha\mu\theta] \neq 0. \tag{4}$$

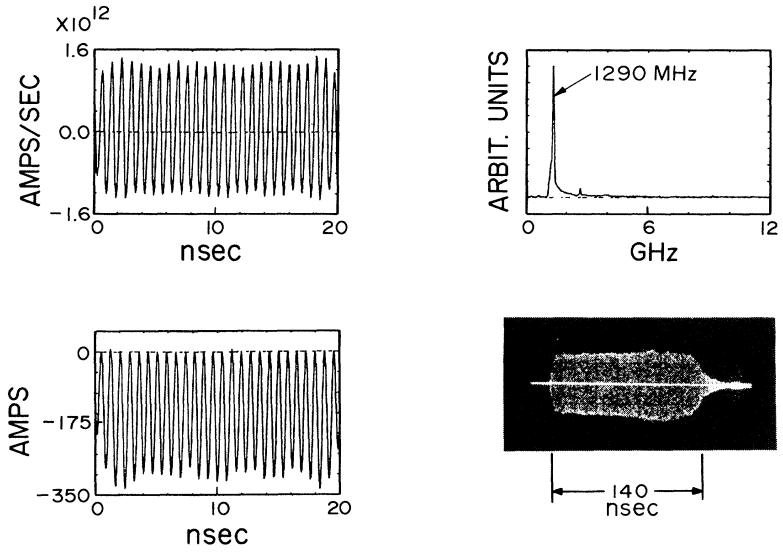

FIG. 2. Experimental results for the arrangement of Fig. 1(a): top left, dI/dt; top right, fast Fourier transform of dI/dt; bottom left, modulated current; bottom right, dI/dt using the 1-GHz Tektronix 7104 oscilloscope—this scope allows the display of the full pulse envelope.

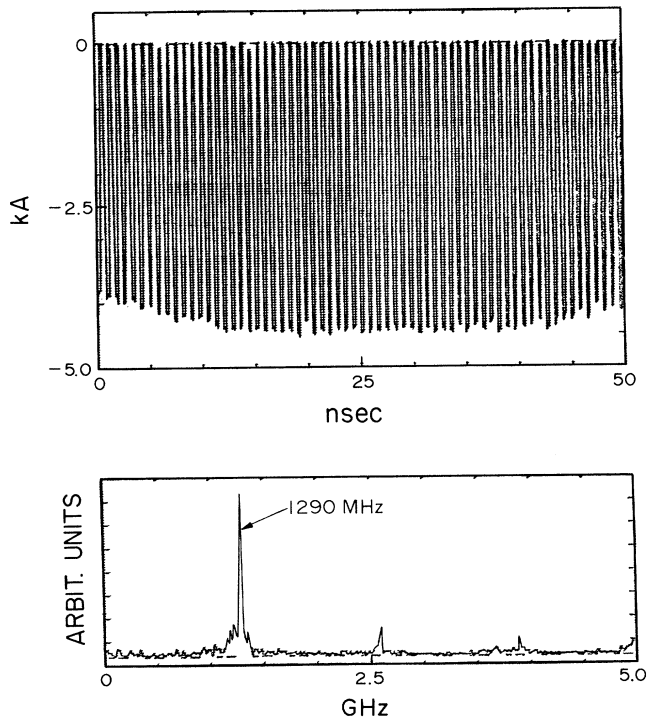

FIG. 3. Experimental results for the arrangement of Fig. 1(b): top, modulated current; bottom, fast Fourier transform of dI/dt.

Equation (4) shows the difference between this mechanism and a "classical klystron mechanism." For a conventional klystron mechanism $P_{ak}=0$ at any point in the drift region, while here $P_{ak}\neq 0$ and $I_2(z,t)\neq 0$ even at $z=0$.

In Eq. (1) the quantity inside the curly brackets is of the order of 1. From the experimental parameters one can calculate that $Z(1-\zeta^2)\approx 35\ \Omega$ and since V_{10} is ≈ 5 kV one gets that $I_2(0,t)\approx 140$ A, or the depth of modulation is ≈ 280 A. This is in excellent agreement with the experimental value of the depth of modulation of 300 A (Fig. 2).

In order to fully modulate the 5-kA IREB one would need to impose on the gap a voltage of ~ 100 kV which is equivalent to the injection of rf power exceeding 20 MW into the present cavity. Instead, we inserted a second cavity in the drift tube 5 cm away from the first one [Fig. 1(b)]. This was a $\lambda/4$ coaxial cavity tuned to 1328 MHz with a characteristic impedance of 45 Ω and $Q\gtrsim 1000$. Voltage oscillations of amplitude $\gtrsim 120$ kV were induced in the second cavity when the partially modulated IREB that emerged from the first cavity traversed it. The emerging IREB from the second cavity was more than 80% modulated at the frequency of 1328 MHz (Fig. 3).

Equation (1) still gives good agreement between the calculated depth of current modulation and the measured one. However, the picture now becomes highly

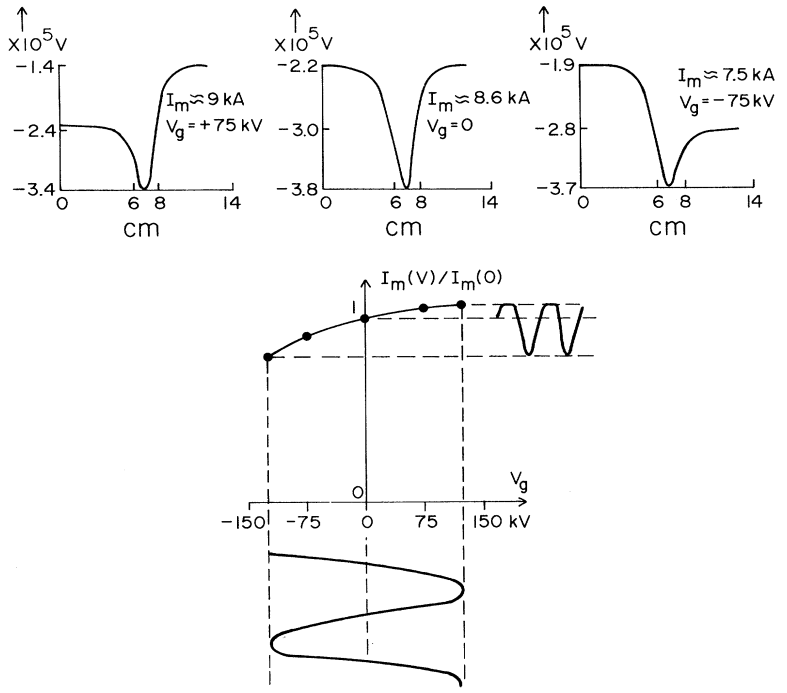

FIG. 4. Top, potential profiles near the gap of the cavity for a current I_m and gap voltage V_g (the gap is located at axial position 6–8 cm). Bottom, dynamic transfer curve showing how the current responds to an oscillating gap voltage.

nonlinear and cannot be explained by slow and fast waves. Usually one uses particle simulation techniques to investigate nonlinear phenomena involving the presence of IREB's. Instead we chose a simpler model that gave us insights into the nonlinear process. This model calculates equipotentials for the geometry of a cavity such as in Fig. 1(a) when a time-independent voltage, V_g, is applied on the gap. The potential, V, is found at any point inside the geometry by solving $\Delta V = -\rho/\epsilon$, with the assumption $\rho u_0 = \text{const}$, where ρ is the electron charge density.

We found that the presence of the gap with the applied voltage influences the maximum IREB current, I_m, that can propagate. Figure 4 shows potential profiles in the vicinity of the gap at the position of the IREB for various gap voltages and for currents close to I_m. Assuming that the IREB flow through the cavity is laminar and that the current is controlled by V_g, one can construct (as for a high-power electron tube) a "dynamic transfer" curve that gives an oscillating current as a response to a sinusoidally time-dependent voltage (Fig. 4, bottom). However, the IREB flow is not laminar and when an oscillating voltage is applied on the gap the following happens: (1) The flow of the IREB is disrupted when $V_g < 0$ and a virtual cathode is formed, reducing the propagating IREB current well below the current I_m calculated above. (2) When $V_g \geq 0$ the virtual cathode disappears and the flow of the IREB is restored to its original level. In the case of a nonlaminar flow of an IREB Fig. 4 (bottom) should be modified by reducing the values of I_m for $V_g < 0$ but keeping the same values of I_m for $V_g > 0$. Hence, an oscillating V_g will induce current oscillations larger than the ones shown in Fig. 4 (bottom). This picture resembles a "classical" electron-tube amplifier with a negatively dc-biased grid. V_g corresponds to the grid ac voltage. When the amplitude of V_g is small compared to the dc grid voltage (the dc grid voltage corresponds to the potential near the gap when $V_g = 0$) the system will behave like a "class A" amplifier; for V_g large enough the system will behave like a "class B" amplifier.

It was shown by us[4,5] that the kinetic energy of a modulated IREB can be converted into rf energy with high efficiency ($\gtrsim 50\%$). Hence, an rf amplifier based on this process will have a gain of $\gtrsim 40$ dB. Note that (1) no optimization of gain and efficiency was attempted and (2) the IREB current was assumed to be sinusoidally modulated; the signals were not corrected for frequencies greater than 1328 MHz.

In conclusion, we showed in this Letter that a relatively low-power rf source modulated an IREB 10^4–10^5 times higher in power, and unlike in conventional klystrons, a long drift length for beam bunching was unnecessary. The modulating frequency was 1.3 GHz but the simple theory presented here and elsewhere[6] predicts that rf radiation of higher frequency (probably $\gtrsim 10$ GHz) could be amplified with similar gain and power levels.

[1]For example, P. B. Wilson, in *Physics of High Energy Accelerators—1981,* edited by R. A. Carrigan, F. R. Huson, and M. Month, AIP Conference Proceedings No. 87 (American Institute of Physics, New York, 1982), pp. 546–550.

[2]R. W. Bierce, J. Jasberg, and J. V. Labacqz, in *The Stanford Two-Mile Accelerator,* edited by R. N. Neal (Benjamin, New York, 1968), Chap. 10.

[3]M. Friedman, V. Serlin, A. Drobot, and Larry Sefort, Phys. Rev. Lett. **50**, 1922 (1983).

[4]M. Friedman, Appl. Phys. Lett. **26**, 366 (1975).

[5]M. Friedman and V. Serlin, Rev. Sci. Instrum. **54**, 1764 (1983).

[6]M. Friedman, V. Serlin, A. Drobot, and Larry Seftor, J. Appl. Phys. **56**, 2459 (1984), and unpublished.

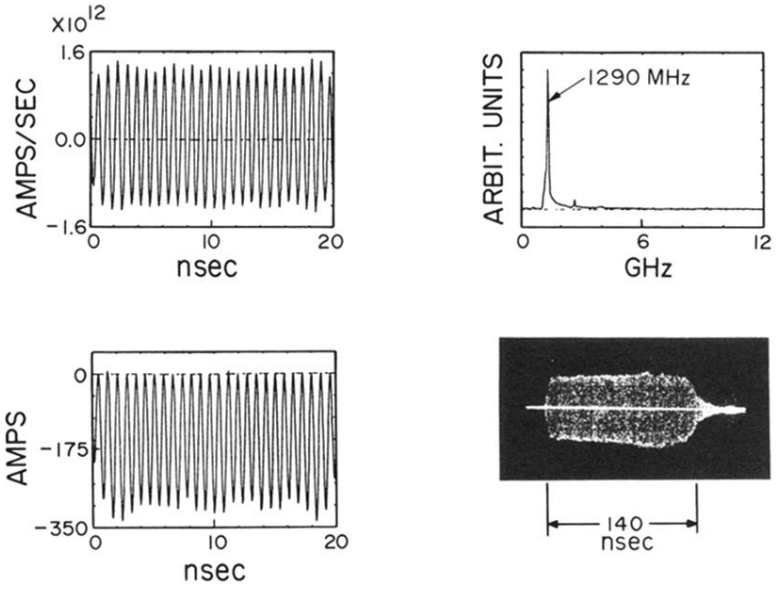

FIG. 2. Experimental results for the arrangement of Fig. 1(a): top left, dI/dt; top right, fast Fourier transform of dI/dt; bottom left, modulated current; bottom right, dI/dt using the 1-GHz Tektronix 7104 oscilloscope—this scope allows the display of the full pulse envelope.